Electronic Supplementary Material (ESI) for RSC Advances.
This journal is © The Royal Society of Chemistry 2022

Supplementary Information for

Polyhedral Oligosilsesquioxane–modified Boron Nitride Enhances the Mechanical Properties of Polyimide Nanocomposites

Yajun Zhang, Jie Wang, Yinjie Chen*

1. Spectral results

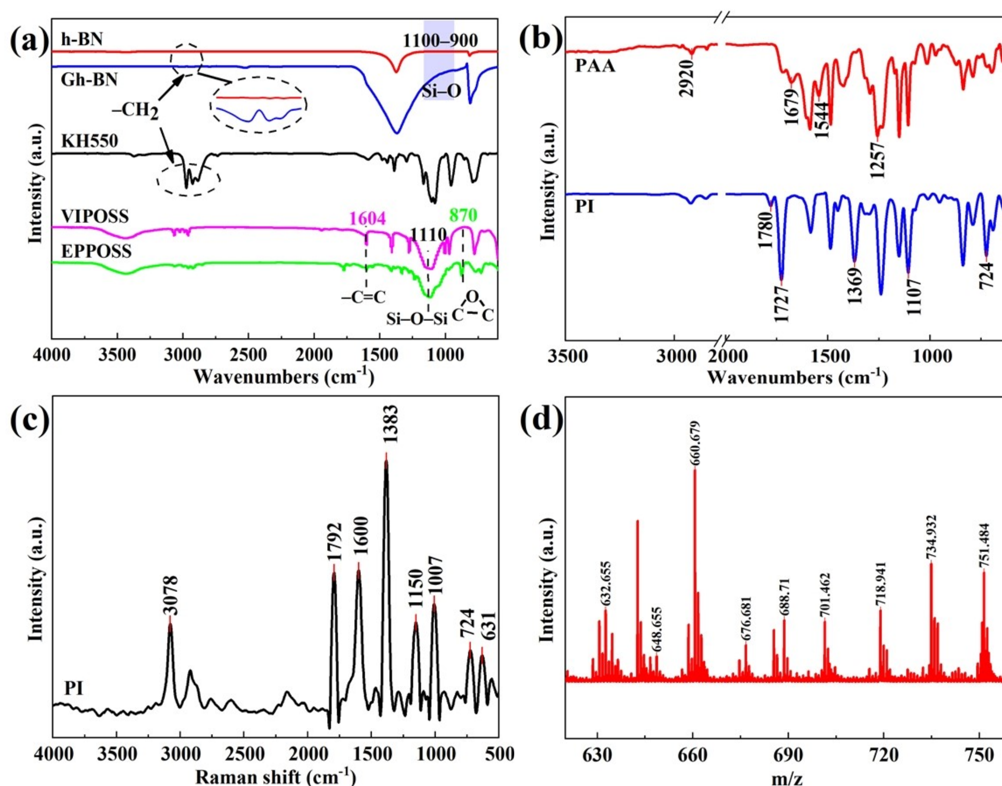

Fig. S1 FTIR spectra of filler (a) and PI films (b); Raman spectrum of PI films (c); Mass spectrum of EPPOSS (d).

As shown in Fig. S1(a), the Gh-BN and KH550 shows two obvious characteristic peaks, corresponding to antisymmetric and symmetric stretching vibration of $-CH_2-$ groups.[1,2] As shown in Fig. S1(b), PAA spectra are compound of the N–H stretch bonds at 2920 cm^{-1}, the C=O carbonyl stretch of the amide I mode around 1679 cm^{-1}, the 1544 cm^{-1} amide II mode, and the 1257 cm^{-1} band due to the C–O–C ether aromatic stretch.[3] After the thermally imidization reaction, the absence of the absorption bands at 1544 cm^{-1} (amide II) and 1679 cm^{-1} (amide I) indicates that PAA has been turned into PI. This is also confirmed by the occurrence of the C=O stretch (imide I) peaks at 1780 cm^{-1} (symmetric) and 1727 cm^{-1} (asymmetric), the typical C–N stretch (imide II) peak around 1369 cm^{-1}, the C–H bend (imide III) and C=O bend (imide IV) absorption bands respectively at 1107 cm^{-1} and 724 cm^{-1}.[4,5] Fig. S1(c) showed the Raman characteristic peaks of the benzene ring in PI are at 3078 cm^{-1}, 1600 cm^{-1}, 1150 cm^{-1}, 1007 cm^{-1}, 724 cm^{-1} and 631 cm^{-1}, and the bands observed at 1792 cm^{-1} and 1383 cm^{-1} are ascribed to symmetrical stretching and contracting vibrations of the carbonyl group (C=O) and C–N stretching vibration of amide ring.[5] Fig. S1(d) shows the mass spectrum of the synthesized EPPOSS sample. The m/z value of 632.655 corresponds to the vinyl POSS (VIPOSS), and 648.655, 660.679, 676.6814, 688.71, 701.462, 718.941, 734.932 and 751.484, correspond to 1, 2, 3, 4, 5, 6, 7 and 8 epoxy groups of epoxy POSS, respectively. Among

them, the content of epoxy POSS with two epoxy groups is higher.

2. SEM images

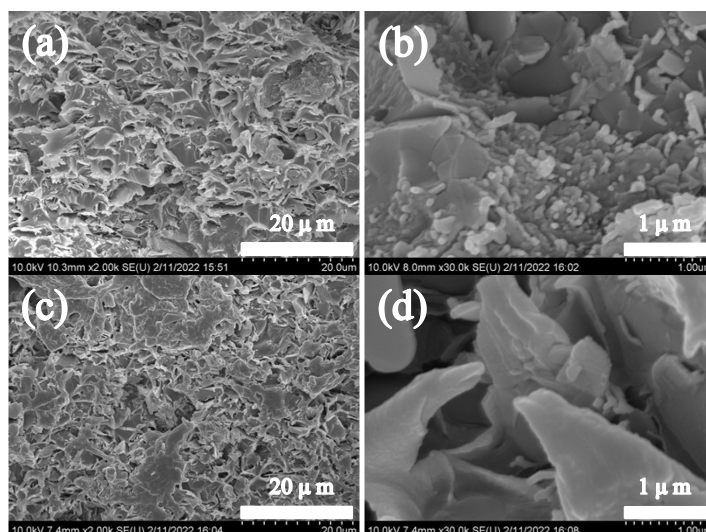

Fig. S2 SEM images of PI nanocompostite films with 3 wt% EPPOSS@Gh-BN (a) and (b); 3 wt% h-BN (c) and (d).

The PI in the fracture interface of the PI/EPPOSS@Gh-BN film is interconnected, with fracture surface branches that are dense and fibre-like, as shown in Fig. S2(a), while the filler and the matrix are in close contact, forming a superimposed state with the PI under the action of EPPOSS, as shown in Fig. S2(b). Fig. S2(c) shows that the PI fracture interface is rough, the h-BN filler contacts the matrix poorly, and the filler orientation is different and irregular.

3. Thickness dependent tensile strength and TGA of PI/EPPOSS@Gh-BN

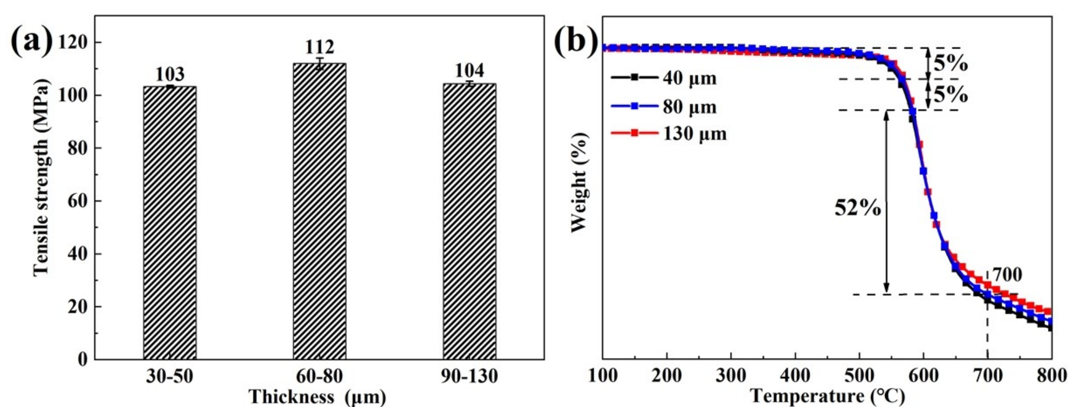

Fig. S3 Thickness dependent tensile strength (a) and TGA (b) curves of PI/EPPOSS@Gh-BN (0.3 wt%).

As shown in Fig. S3, the mechanical and thermal properties of PI/EPPOSS@Gh-BN (0.3 wt%) nanocomposite films with various thicknesses were analyzed. The tensile strength of the three thicknesses show the order of 60-80 μm ＞ 90-130 μm ＞ 30-50 μm (Fig. S3(a)). The thermal properties of the three thicknesses show similar trend (Fig. S3(b)). The weight loss temperatures of the PI/EPPOSS@Gh-BN nanocomposite fillers increase with the thickness increase within 10% thermal weight loss. At 700 °C, the residual mass ratio of the PI/EPPOSS@Gh-BN nanocomposite films with a thickness of 130 μm was slightly larger than that thicknesses of 80 μm and 40 μm, respectively.

4. DSC and DMA analysis

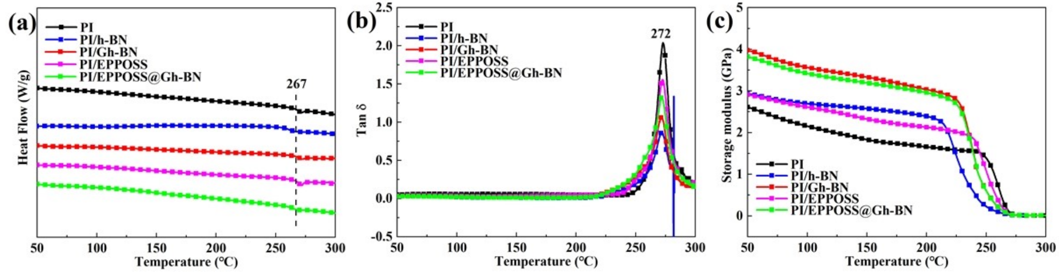

Fig. S4 Thermal performance of PI nanocomposite films. DSC: (a); DMA: (b) and (c).

Fig. S4(b) and (c) show the typical dynamical mechanical analysis (DMA) curves of the PI, PI/h-BN (0.2 wt%), PI/Gh-BN (0.2 wt%), PI/EPPOSS (0.1 wt%) and PI/EPPOSS@Gh-BN (0.3 wt%) nanocomposite films. Glass-transition temperatures (T_g) were an important factor in evaluating the thermal properties of polymers. Fig. S4(b) shows the temperature dependence of tan δ of the PI and PI nanocomposite films. The T_g of the pure PI was 272 °C. The addition of a low content of Gh-BN, EPPOSS or nanocomposite fillers did not show favorable effect on T_g of the PI, this is consistent with the differential scanning calorimetry (DSC) curves in Fig. S4(a). As shown in Fig. S4(c), the storage modulus of pure PI was the lowest in those PI nanocomposite films, while the PI/EPPOSS@Gh-BN and PI/Gh-BN have a comparatively higher storage modulus of 4 GPa at room temperature due to the addition of the hard ceramic BN fillers in the PI polymer.

5. CTE analysis

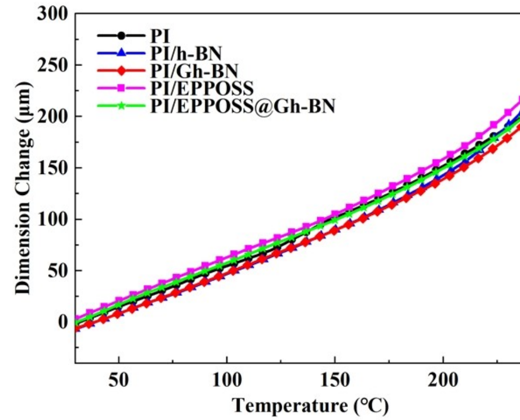

Fig. S5 TMA curves of PI nanocomposite films. CTE_{PI}: 6.35×10^{-5} /°C; $CTE_{PI/h\text{-}BN}$: 6.79×10^{-5} /°C; $CTE_{PI/Gh\text{-}BN}$: 6.26×10^{-5} /°C; $CTE_{PI/EPPOSS}$: 6.77×10^{-5} /°C; $CTE_{PI/EPPOSS@Gh\text{-}BN}$: 6.33×10^{-5} /°C.

The coefficient of thermal expansion (CTE) values of the current PI and PI nanocomposite films in the temperature ranges between 25 to 250 °C were evaluated through thermal mechanical analysis (TMA) measurements. The CTE value is crucial for its dimensional stability, and the results are shown in Fig. S5. The CTE values of PI/Gh-BN (CTE = 6.26×10^{-5} /°C) films were lower than that of PI/h-BN and pure PI, respectively, which is because the surface modification on Gh-BN leads to the stronger interaction between the two phases. Therefore, the CTE of the PI/Gh-BN film can be further reduced. The PI/EPPOSS film showed the CTE value of 6.77×10^{-5} /°C, which is slightly higher than that of the pure PI (CTE = 6.35×10^{-5} /°C) film due to the internal plasticization effects of the latent POSS units in the PI.[6] While the CTE of PI/EPPOSS@Gh-BN (CTE = 6.33×10^{-5} /°C) is marginally lower than that of pure PI, which is because of the improved chain orientation of PI by Gh-BN. This suppresses the thermal expansion of the PI matrix.[7] The reduction of the CTE value of the PI nanocomposite film can weaken the thermal stress of the PI and the copper clad laminate during the hot pressing process, and prevent the PI/Cu laminate from curling.[8]

6. Contact angle

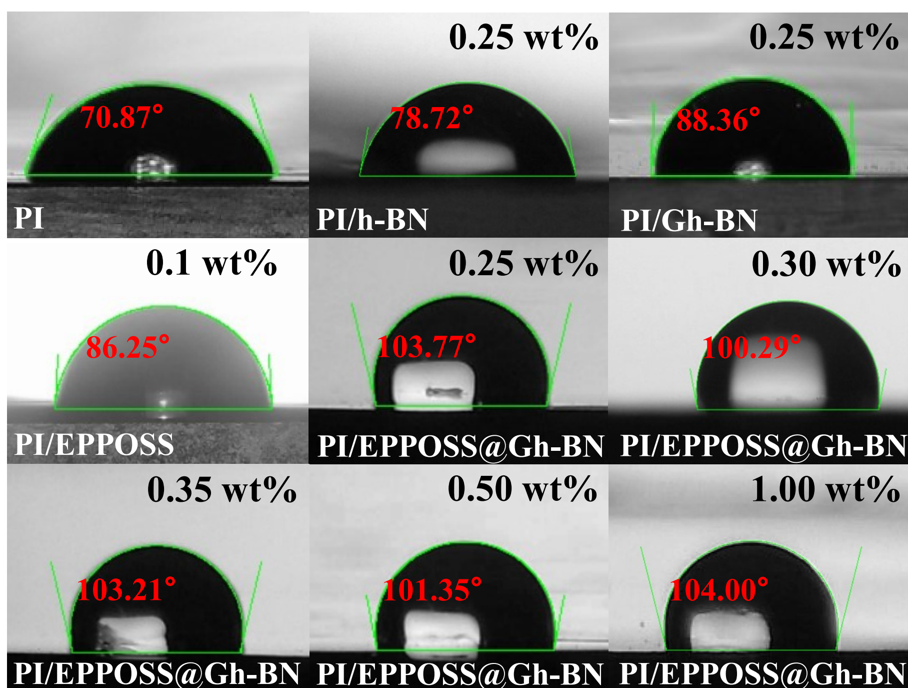

Fig. S6 Contact angle pictures of PI nanocomposite films.

7. Optical properties

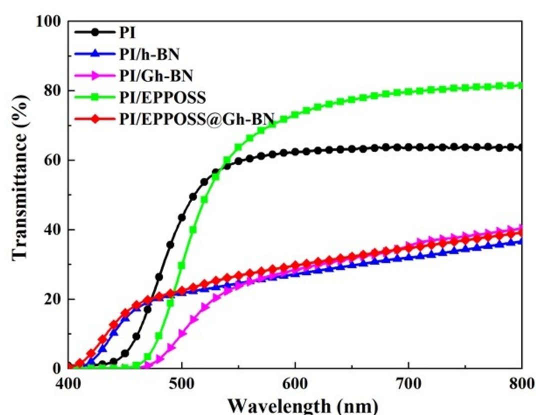

Fig. S7 UV–Vis spectra of the PI nanocomposite films from 400 to 800 nm wavelength.

The optical transparency of PI composition films was measured with UV–Vis spectroscopy. Fig. S7 shows that the PI/EPPOSS (0.1 wt% EPPOSS) film has highest transmittance of 81%, which exceeds pure PI at 540–800 nm. PI/h-BN (0.25 wt% h-BN), PI/Gh-BN (0.25 wt% Gh-BN) and PI/EPPOSS@Gh-BN (0.25 wt% Gh-BN and 0.1 wt%) have poor light transmittance due to the nonlinear optical properties of hexagonal boron nitride.[9]

References

1 Y. Fan, H. Yang, H. Fan, Q. Liu, C. Lv, X. Zhao, M. Yang, J. Wu and X. Cao, *Materials (Basel)*, 2020, **13**, 2340.

2 C. Chen, J. Wang, X. Chen, X. Yu and Q. Zhang, *High Perform. Polym*., 2018, **31**, 294–303.

3 S. Diaham, M. L. Locatelli, T. Lebey and D. Malec, *Thin Solid Films*, 2011, **519**, 1851–1856.

4 H. Seo, B. Chae, J. H. Im, Y. M. Jung and S. W. Lee, *J. Mol. Struct*., 2014, **1069**, 196–199.

5 H. Ishida, S. T. Wellinghoff, E. Baer and J. L. Koenig, *Macromolecules*, 1980, **13**, 826–834.

6 H. Wu, Y. Zhang, Y. Guo, H. Qi, Y. An, Y. Jia, Y. Tan, J. Liu and B. Wu, *Polymers*, 2020, **12**, 2865.

7 M. Tsai, I. Tseng, J. Chiang and J. Li, *ACS Appl. Mater. Interfaces*, 2014, **6**, 8639-8645.

8 X. M. Zhang, X. Xiao, X. Wu and J. G. Liu, *Express Polym. Lett.*, 2017, **11**, 983-990.

9 P. Kumbhakar, A. K. Kole, C. S. Tiwary, S. Biswas, S. Vinod, J. Taha-Tijerina, U. Chatterjee and P. M. Ajayan, *Adv. Opt. Mater.*, 2015, **3**, 828–835.